

Droplets moving on a fluid surface: interference pattern from two slits

Valeriy I. Sbitnev*

*B. P. Konstantinov St. Petersburg Nuclear Physics Institute,
NRC Kurchatov Institute, Gatchina, Leningrad district, 188350, Russia;
Department of Electrical Engineering and Computer Sciences,
University of California, Berkeley, Berkeley, CA 94720, USA*

(Dated: August 16, 2018)

The Feynman path integral approach for solving the motion of a droplet along a silicon oil surface is developed by replacing the Planck constant by a surrogate parameter. The latter is proportional to the surface tension of the silicon oil multiplied by the area of the thin air film, separating the droplet from the oil, and by the half-period of the Faraday oscillations. It is shown that the Navier-Stokes equation together with the mass conservation equation can be reduced to the Schrödinger equation when the surrogate parameter replaces the Planck constant. The Feynman path integral underlying the Schrödinger equation is used then to calculate a wave function that plays the role of the de Broglie pilot-wave.

Keywords: Faraday waves; droplet; Navier-Stokes; Schrödinger; Feynman path integral; wave function; probability density; Bohmian trajectory; interference

I. INTRODUCTION.

Recently a team of French scientists has shown that oil droplets on the "silicon oil - air" interface can behave as quantum particles, demonstrating the interference phenomenon from two slits [1]. Behavior of the droplets leads to the emergence of amazing structures [2–4], appearance of which is typical for self-organization of interacting atoms as quantum objects. One more quantum-mechanical analogy is the creation of a pair "drop - anti-drop" as a result of the collision of two solitary waves [5], Fig. 1, thus simulating the phenomenon of "electron-positron" pair creation. Feynman diagram technique [6] involving operators of creation and annihilation of different harmonic modes [7, 8] can be used in the same manner in order to observe the creation/annihilation of drop-anti-drop pairs.

Generating Faraday waves by vertically vibrating bath is an indispensable part in such experiments [1–4, 9–11]. Note that these waves are slightly below the bifurcation threshold. Such oscillations can be imagined to be akin to vacuum zero-point oscillations. In other words, the motion of droplets on such surfaces may imitate the motion of particles in the vacuum, Fig. 2.

Notwithstanding the similarity with quantum-

mechanical phenomena we cannot apply quantum formulas to describe the observed motion first of all because of the smallness of the main quantum constant - the Planck constant $h \sim 10^{-34}$ J·s. The formula $\Delta E \Delta t = \hbar$ can relate to the exchange of energy with the virtual particles of quantum vacuum, not with the sub-critical Faraday oscillations. Droplets are heavy objects having a mass about $m \sim 1$ mg and moving with velocities about 10 mm/s [2]. Formally, we can evaluate that wavelength of such droplets would be about 10^{-23} mm. From here it follows that the Planck constant cannot be adopted as a native constant for the droplet interference experiments. Instead, we need to use a surrogate parameter, η_σ , replacing the Planck constant, Fig. 2.

Let us recall experiment with silicon droplets [1]. A bouncing droplet rests on the fluid surface divided by a thin air film which prevents coalescence of the droplet with the fluid in the bath [2] (it is akin to retention of water striders on a water surface due to surface tension). So, the surface tension of the silicon oil, $\sigma = 0.0209$ N/m [3], can be the main parameter determining the surrogate parameter. On the other hand, the droplet rests on the basic fluid substance of a small area, ΔS , restricted by a solid angle Ω , Fig. 1(d). The energy consumed to support the droplet on the fluid surface for duration of bouncing, Δt , is $\Delta E = \sigma \Delta S$. From

*Electronic address: valery.sbitnev@gmail.com

here it follows, that the surrogate parameter, η_σ , can have the following form

$$\eta_\sigma = \Delta E \Delta t = \sigma \Delta S T_0 / 2. \quad (1)$$

Here $\Delta t = T_0/2$ is a half-period of the Faraday oscillations of the fluid generated by an external vibrator [1]. Estimation gives $\eta_\sigma \sim 10^{-11}$ J·s for ΔS being represented by 0.05 part of the surface area of a sphere of a droplet having diameter about 0.76 mm [4] and a period of the Faraday oscillations $T_0 \sim 12$ ms (the forcing frequency is 80 Hz [4]). Now we may evaluate a wavelength of the droplet, λ , having mass $m \sim 0.2$ mg and moving with a velocity, v_z , of about 10 mm/s. It is about $\eta_\sigma / mv_z = 5$ mm. This wavelength is in a good agreement with that given in [1, 4].

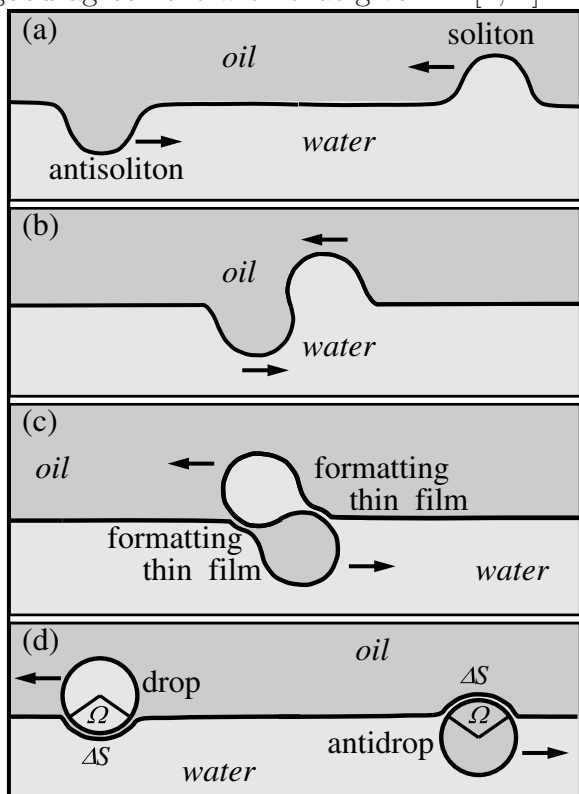


FIG. 1: Creation of the pair "drop-anti-drop" as a result of collision of two solitary waves on the interface of media "oil-water" [5]: (a) two solitary waves, soliton and antisoliton, move to meet each other; (b) moment of their collision; (c) formation of thin films between droplets and fluids; (d) droplet and anti-droplet are separated from fluids by thin films with area about ΔS .

By adopting the parameter η_σ as a quantum of action we show that the Navier-Stokes equation together with the mass conservation equation has a close relation to the Schrödinger equation,

where the Planck constant should be replaced by this parameter. Next we calculate the Feynman path integral for the motion of droplets through a double-slit grating. Calculations disclose an interference pattern behind the grating and a set of Bohmian trajectories along which the motion of the droplets occurs.

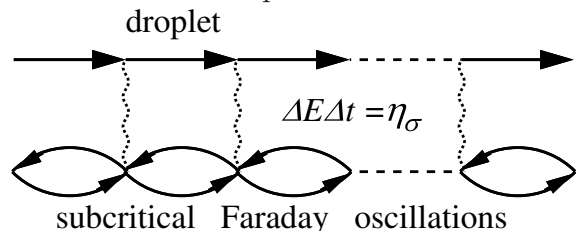


FIG. 2: Feynman-like diagram representing the motion of a droplet bouncing along the silicon oil surface. Exchange by energy via a generated surface wave occurs at each bounce. Here relation $\Delta E \Delta t = \eta_\sigma$ simulates the quantum-mechanical relation $\Delta E \Delta t = \hbar$. Similar diagram technique [6] involving operators of creation and annihilation of different harmonic modes [7, 8] can be used in order to observe the creation/annihilation of drop-anti-drop pairs.

II. TRANSFORMATION OF THE NAVIER-STOKES EQUATIONS.

Quantum theory in a hydrodynamic form was formulated by Erwin Madelung in 1926 [12] as an alternative formulation of the Schrödinger equation. Remarkably that Madelung's equations exhibit a close relationship through the Bohmian mechanics [13, 14] with hydrodynamic equations such as the Navier-Stokes equations. It gives the reason to hypothesize that quantum medium behaves like a fluid with irregular fluctuations [15]. On the other hand, we may suppose that behavior of an incompressible liquid can be described by a Schrödinger-like equation with a special parameter replacing the Planck constant. Let us trace this supposition.

Two equations, describing flow of an incompressible fluid, are [16]:

(a) the Navier-Stokes equation

$$\rho_M \left(\frac{\partial \vec{v}}{\partial t} + (\vec{v} \cdot \nabla) \vec{v} \right) = -\nabla P + \mu \nabla^2 \vec{v} + \frac{\vec{F}}{\Delta V}, \quad (2)$$

(b) the mass conservation equation

$$\frac{\partial \rho_M}{\partial t} + \nabla \cdot (\rho_M \vec{v}) = 0. \quad (3)$$

Here \vec{v} is a flow velocity, P is a pressure, μ is the viscosity coefficient, and $\vec{F}/\Delta V$ is a force per unit volume ΔV . A mass density ρ_M is defined as the mass of the fluid, M , per volume ΔV :

$$\rho_M = \frac{M}{\Delta V} = \frac{mN}{\Delta V} = m\rho. \quad (4)$$

Next we shall represent M as a product of an elementary mass m by the number of these masses, N , contained within volume ΔV . Then the mass density ρ_M can be defined as a product of the elementary mass m by the density of elementary carriers, $\rho = N/\Delta V$. The elementary carrier is a droplet-like inhomogeneity, which moves with the local stream velocity of the equivalent fluid. We assume that each elementary carrier of mass m is subjected to the Brownian motion with a diffusion coefficient inversely proportional to m and no friction [17]. In this sense, ρ represents a probability density of finding the carrier within the volume ΔV and obeys the conservation law (3).

As for the term $(\vec{v} \cdot \nabla)\vec{v}$ in Eq. (2), it can be rewritten as $(\vec{v} \cdot \nabla)\vec{v} = \nabla v^2/2 - [\vec{v} \times [\nabla \times \vec{v}]]$. Further we shall consider irrotational flows, that is, $[\nabla \times \vec{v}] = 0$. Let the force be conservative, $\vec{F} = -\nabla\mathcal{U}$. In this case we rewrite the Navier-Stokes equation in the following form

$$m\frac{\partial \vec{v}}{\partial t} + m\nabla\frac{v^2}{2} - \frac{\nabla P}{\rho} + \frac{\mu}{\rho}\nabla^2\vec{v} - \frac{\nabla\mathcal{U}}{\rho\Delta V}. \quad (5)$$

The rightmost term, $-\nabla\mathcal{U}/\rho\Delta V = -\nabla U$, is the force acting on the elementary carrier.

One can see that $m\vec{v}$ is a momentum of the elementary carrier and $mv^2/2$ is its kinetic energy. Let us define these quantities through introducing action S - a mathematical functional which accounts for the history of the system in the Lagrangian mechanics [13, 14]:

$$\vec{p} = m\vec{v} = \nabla S, \quad (6)$$

$$m\frac{v^2}{2} = \frac{1}{2m}(\nabla S)^2. \quad (7)$$

Substituting these expressions in the Navier-Stokes equation (5) we obtain

$$\nabla\left(\frac{\partial S}{\partial t} + \frac{1}{2m}(\nabla S)^2 + U + Q\right)$$

$$= -\frac{\nabla P}{\rho} + \frac{\mu}{\rho}\nabla^2\vec{v} + \nabla Q. \quad (8)$$

We have added gradient of the term

$$Q = -\frac{\eta_\sigma^2}{2m}\left[\frac{\nabla^2\rho}{2\rho} - \left(\frac{\nabla\rho}{2\rho}\right)^2\right] \quad (9)$$

to both sides of Eq. (8). If η_σ will be substituted by \hbar , the term Q will represent the quantum potential first defined by D. Bohm [18].

Right hand side (RHS) of Eq. (8) besides the pressure force and the viscosity force contains also the term (9). Under the assumption of incompressibility, the density of the elementary fluid volume is constant. It stays below the Faraday instability threshold. From here we can assume that the gradient of ρ is zero and we may omit the gradient operator in Eq. (8). RHS, free from the gradient, looks as

$$-\frac{P}{\rho} + \frac{\mu}{\rho}\nabla\vec{v} - \frac{\eta_\sigma^2}{2m}\left[\frac{\nabla^2\rho}{2\rho} - \left(\frac{\nabla\rho}{2\rho}\right)^2\right] = -V_N. \quad (10)$$

The Fick's law says that the diffusion flux, J , is proportional to the negative value of the density gradient, $J = -(D/2)\nabla\rho$, where $D = \eta_\sigma/2m$ is the diffusion coefficient [17]. The term $\eta_\sigma\nabla J$ has dimensions of the pressure. From here it follows that the pressure P has a diffusion nature

$$P = \eta_\sigma\nabla J = -\frac{\eta_\sigma^2}{4m}\nabla^2\rho. \quad (11)$$

By substituting this expression in Eq. (10) we have

$$V_N = -\frac{\eta_\sigma^2}{2m}\left(\frac{\nabla\rho}{2\rho}\right)^2 - \frac{\mu}{m\rho}\nabla^2 S. \quad (12)$$

By integrating Eq. (8) over the volume of the fluid we get

$$\frac{\partial S}{\partial t} + \frac{1}{2m}(\nabla S)^2 + U + V_N - \frac{\eta_\sigma^2}{2m}\left(\frac{\nabla^2\rho}{2\rho}\right) + \frac{\eta_\sigma^2}{2m}\left(\frac{\nabla\rho}{2\rho}\right)^2 = C, \quad (13)$$

$$\frac{\partial \rho}{\partial t} + \nabla(\rho \cdot \vec{v}) = 0. \quad (14)$$

Here we wrote down also the continuity equation for the probability density ρ . In Eq. (13) C is an integration constant.

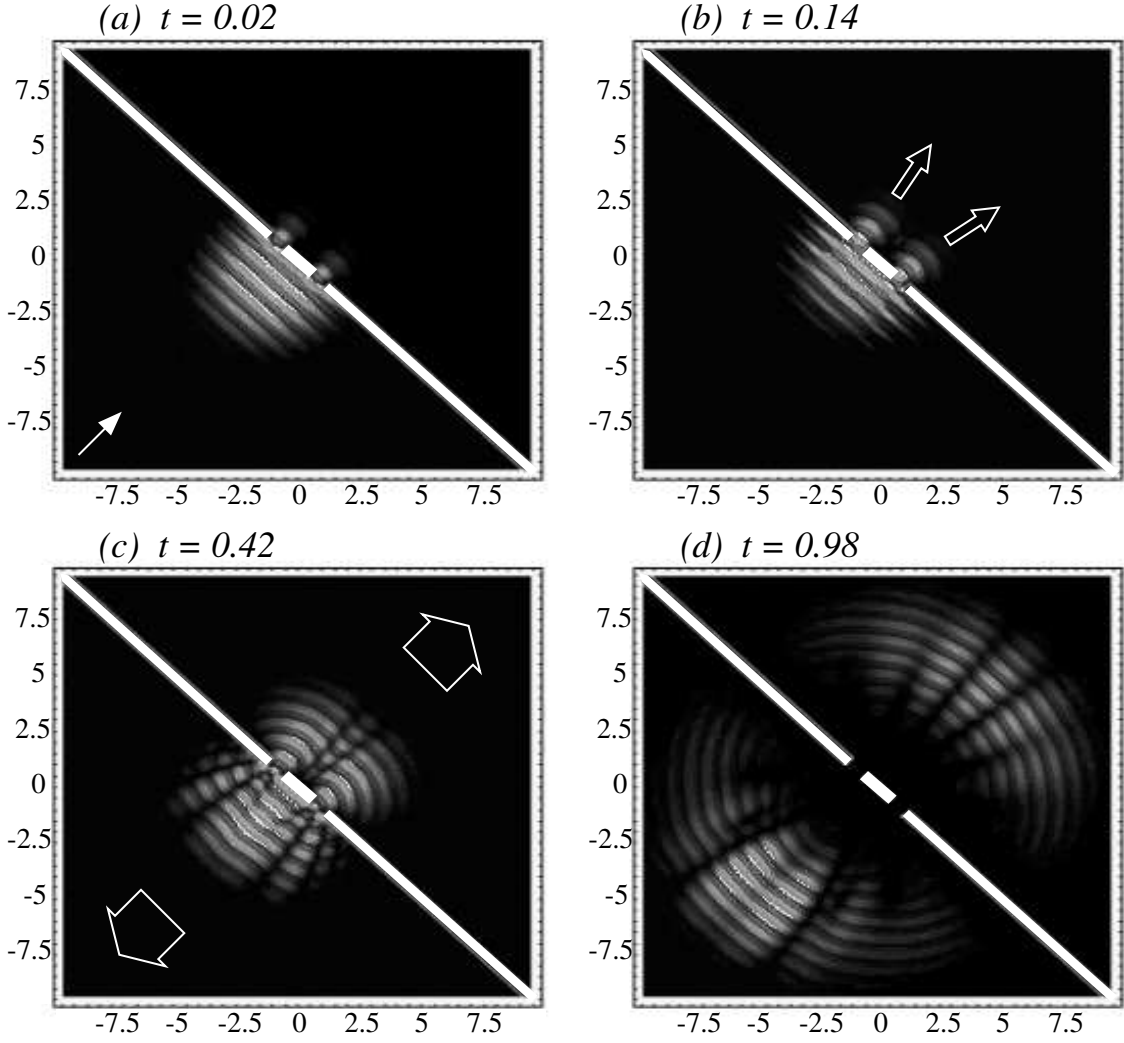


FIG. 3: Scattering of a Gaussian soliton-like wavepacket on a barrier containing two slits [19]. Time here is in seconds and scale of the area is given in centimeters. Velocity of the wave is about 150 mm/s. It corresponds to the phase velocity of the Faraday waves [1].

The modified Hamilton-Jacobi equation (13) with extra terms and the continuity equation (14) stems from a nonlinear Schrödinger like equation

$$\mathbf{i}\eta_\sigma \frac{\partial \Psi}{\partial t} = -\frac{\eta_\sigma^2}{2m} \Delta \Psi + U\Psi + V_N\Psi - C\Psi. \quad (15)$$

Nonlinearity arises due to the term V_N that depends on both ρ and S . Note that the wave function Ψ written down in a polar form contains exactly these functions

$$\Psi = \sqrt{\rho} \exp\{\mathbf{i}S/\eta_\sigma\}. \quad (16)$$

By substituting this function in Eq. (15) and by separating real and imaginary parts, we obtain Eqs. (13) and (14).

Due to the assumption that the fluid is incompressible and below the Faraday instability threshold, the term V_N in Eq. (13) can be omitted. We come to the linear Schrödinger equation. A solution of the linear Schrödinger equation with the potential simulating a barrier with two slits [19] is shown in Fig. 3. Scattering of a Gaussian soliton-like wave on the slits produces two waves - reflected and transmitted. Both waves evolve against the background of subcritical Faraday waves. Similar interference manifestation of waves on the water surface can be found on YouTube. Here is one [20].

As for the Faraday waves, Eq. (15) under conditions stated in [9, 10] reduces to the Miles-Henderson wave equation describing theirs.

III. MOVING DROPLET IN TERMS OF THE PATH INTEGRAL.

Note that the Schrödinger equation can be deduced from the Feynman path integral [21] by successive expansion in a Taylor series of kernels of this integral [22, 23]. It means that along with the Schrödinger equation the path integral can be used for consideration of a moving droplet through slits [1]. A main step here is the re-

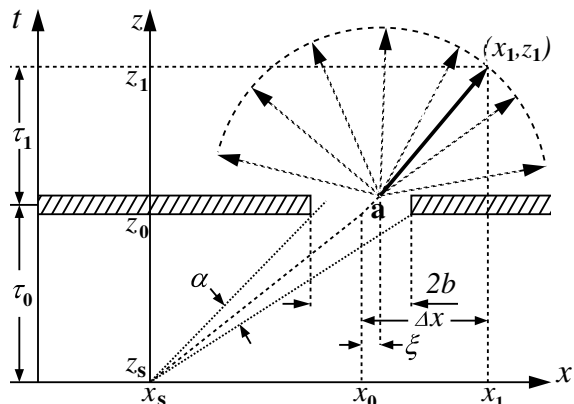


FIG. 4: Single slit is localized in the vicinity of point x_0 on a grating situated at distance $z_0 - z_s$ away from a source. A droplet, emitted by the source in the vicinity of point (x_s, z_s) , moves along a path within a ray α to the slit and further along some path pointed to by arrows.

placement of the Planck constant \hbar in the path integral by the surrogate parameter η_σ equal to 1.185×10^{-11} J·s in our case. Its value is evaluated for a case of the forcing frequency $f_0 = 80$ Hz and the droplet diameter $D = 0.76$ mm [4].

From here it follows that at $\rho_M = 965$ kg/m³ the mass of the droplet is $m = \rho_M(4/3)\pi(D/2)^3 \sim 0.22$ mg. Let us begin from presentation of a Lagrange function that describes the free motion of the droplet from a source localized at (x_s, z_s) through (x_1, z_1) within a slit and further to a zone of detection, (x_2, z_2) , as shown in Fig. 4. There is no any interaction with other droplets. The Lagrange function of the free motion is

$$L = m\frac{\dot{x}^2}{2} + \text{const.} \quad (17)$$

Here m is the mass of the droplet and \dot{x} is its transversal velocity. Its longitudinal velocity, v_z , can take values from 1 mm/s up to 20 mm/s [1]. By moving the droplet by a small distance $\delta x = (x_b - x_a) \ll 1$ in the transversal direction, performed for a small time increment $\delta t = (t_b - t_a) \ll 1$, we write down a weight factor $\exp\{\mathbf{i}S/\eta_\sigma\} = \exp\{\mathbf{i}L\delta t/\eta_\sigma\}$ of the path integral in the following form [22]

$$e^{\mathbf{i}L\delta t/\eta_\sigma} = \exp\left\{\frac{\mathbf{i}m(x_b - x_a)^2}{2\eta_\sigma(t_b - t_a)}\right\} \quad (18)$$

The path integral computes probability amplitude that is equal to integral convolution of two kernels, each describing the motion of the free particle (the first describes the motion from the source to the slit, and the second describes the motion behind the slit, Fig. 4:

$$\psi(x_1, x_0, x_s) = \int_{-b}^b K(x_1, \tau_0 + \tau_1; x_0 + \xi, \tau_0) K(x_0 + \xi, \tau_0; x_s, 0) d\xi. \quad (19)$$

The kernel consists of the weight factor (18) multiplied by an amplitude factor [22]

$$K(x_b, t_b; x_a, t_a) = \left[\frac{2\pi\mathbf{i}\eta_\sigma(t_b - t_a)}{m}\right]^{-1/2} \cdot \exp\left\{\frac{\mathbf{i}m(x_b - x_a)^2}{2\eta_\sigma(t_b - t_a)}\right\}. \quad (20)$$

After all computations of the path integral in approximation of the slit by a single Gaussian curve [24], we find a wave function from a single slit

$$\psi(x_1, z_1, x_0, z_0, x_s, z_s) = \sqrt{\frac{m}{2\pi\mathbf{i}\eta_\sigma\tau_0\tau_1}} \left(\frac{1}{\tau_1} + \frac{1}{\tau_0} + \mathbf{i}\frac{\eta_\sigma}{mb^2}\right)^{-1/2}$$

$$\times \exp \left\{ \frac{\mathbf{i}m}{2\eta_\sigma} \left(\frac{(x_1 - x_0)^2}{\tau_1} + \frac{(x_0 - x_0)^s}{\tau_0} - \frac{((x_1 - x_0)/\tau_1 - (x_0 - x_0)/\tau_0)^2}{(1/\tau_1 + 1/\tau_0 + \mathbf{i}\eta_\sigma/mb^2)} \right) \right\} \quad (21)$$

Here the time values, τ_0 and τ_1 , relate to the coordinates z_s, z_0, z_1 according to the following formulas: $\tau_0 = (z_0 - z_s)/v_z$ and $\tau_1 = (z_1 - z_0)/v_z$, see Fig. 4.

For the sake of simplicity we remove the source to negative infinity. In this case τ_0 tends to infinity and the amplitude factor $A = (m/2\pi\mathbf{i}\eta_\sigma\tau_0\tau_1)^{1/2}$ tends to zero (luminosity of a remote source tends to zero). In the paraxial approximation (sources of the droplets are removed to infinity, but A remains finite) the wave function looks as [25, 26]

$$\psi(x, z, x_0, z_0) = A\Sigma_S^{-1/2} \exp \left\{ \mathbf{i}\pi \frac{(x - x_0)^2}{\lambda(z - z_0)} \left(1 - \frac{1}{\Sigma_S} \right) \right\}. \quad (22)$$

Here A is the amplitude factor and the term

$$\Sigma_S = 1 + \mathbf{i} \frac{\lambda(z - z_0)}{2\pi b^2} \quad (23)$$

is a dimensionless complex-valued distance-dependent spreading which relates closely to the complex-valued time-dependent spreading [27, 28]. Note that instead of parameters m, v_z , and η_σ a wavelength $\lambda = \eta_\sigma/mv_z$ appears in Eqs. (22)-(23). Also in Eq. (23) b is half-width of the slit. Hereinafter we omit subscript 1: $(x_1, z_1) \rightarrow (x, z)$. Therefore (x_0, z_0) and (x, z) describe the location of the center of the grating and a position of the detecting droplet, respectively. Now we can write down a general wave function from the grating as superposition of the wave functions (22) from N slits:

$$|\Psi(x, z)\rangle = \frac{1}{N} \sum_{k=-\frac{N-1}{2}}^{\frac{N-1}{2}} \psi(x - kd, z). \quad (24)$$

Here d is the distance between the slits. In case of even number of the slits, $N = 2K$, k runs $-K + 1/2, -K + 3/2, \dots, -1/2, 1/2, \dots, K - 3/2, K - 1/2$. For odd number, $N = 2K + 1$, k runs $-K, -K + 1, \dots, -1, 0, 1, \dots, K - 1, K$. We have chosen here a reference frame with the origin placed in $x_0 = 0$ and $z_0 = 0$.

Probability density function in the vicinity of the observation point (x, z) reads

$$p(x, z) = \langle \Psi(x, z) | \Psi(x, z) \rangle. \quad (25)$$

In order to evaluate these computations we shall consider scattering of droplets on a grating containing two slits, $N = 2$, with $d = 6b$ and the width of the slits $2b = 10$ mm. These param-

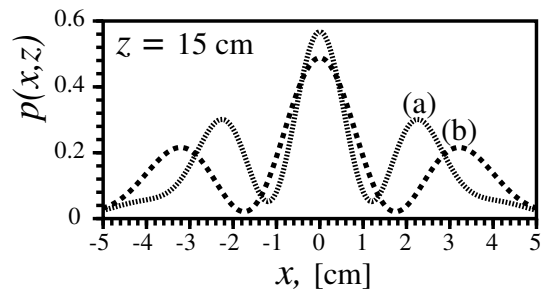


FIG. 5: Interference fringes in a cross-section of the probability density $p(x, z)$ in the far-field, $z = 15$ cm, : (a) $\lambda = 4.75$ mm; (b) $\lambda = 6.95$ mm.

eters will be fixed for all wavelengths in order to compare any output data. Two wavelengths, $\lambda = 4.75$ mm and $\lambda = 6.95$ mm [1, 4], are chosen for subsequent consideration. Cross-sections of the probability density function disclose interference fringes in the far-field, Fig. 5, arising after passing droplets through an obstacle with two slits. The two curves, (a) for $\lambda = 4.75$ mm and (b) for $\lambda = 6.95$ mm, show qualitative accordance with those presented in [1]. One can see that as the wavelength increases the fringes diverge apart. There is, however, some discrepancy. It is due to the fact that the formula in [1] describes amplitude of the diffraction, whereas Eq. (25) relates to description of the intensity. In fact, we need to square an observed amplitude in order to get a clear description of the interference pattern in the far-field [25].

As follows from observations [4] a droplet induces a wave on surface of the oil at the time of each rebound. The wave retains memory about

previous impacts of the droplet and corrects its subsequent motion. It is a manifestation of the effect of the de Broglie pilot-wave that guides the droplet along an optimal path. In our case the wave function $|\Psi(x, z)\rangle$ represents the de Broglie pilot-wave, and the optimal path is called the Bohmian trajectory [13, 14]. Velocity of a shift of the droplet in the plane (x, z) is computed from Eq. (6)

$$\dot{\vec{r}} = \frac{1}{m} \nabla S = \frac{\eta_\sigma}{m} \Im[\Psi^{-1} \nabla \Psi]. \quad (26)$$

The wave function represented in a polar form, $\Psi = R \cdot \exp\{\mathbf{i}S/\eta_\sigma\}$, verifies this formula. Here

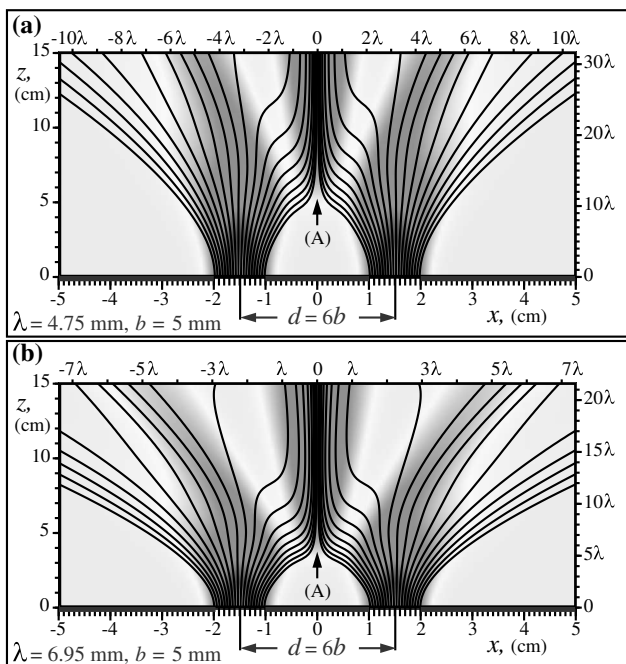


FIG. 6: Bohmian trajectories going out from two slits are shown by black curves against the background of the probability density depicted by gray (light gray refers to low density; dark gray refers to high density): (a) $\lambda = 4.75$ mm; (b) $\lambda = 6.95$ mm. Arrows (A) point to places where Bohmian trajectories dramatically change direction.

R is its amplitude and S divided by η_σ is a phase. Knowing the velocity from Eq. (26) we can find a mean value of the optimal path [26] - the Bohmian-like trajectory. The trajectories are shown in Figs. 6(a) and 6(b) by black curves against the background of the probability density colored in gray (it ranges from light gray (low density) to dark gray (high density)). Fig. 6(a) shows a bundle of the trajectories for the case of $\lambda = 4.75$ mm; the current veloc-

ity, $\eta_\sigma/(\lambda m)$, is about 11 mm/s. Fig. 6(b) shows a bundle of the trajectories for the case of $\lambda = 6.95$ mm; the current velocity is about 8 mm/s. One can see that at the increasing wavelength the trajectories diverge apart considerably stronger for the same path length along z . One can see, in particular, that for observation of the interference effects, the size of the bath can be about 10×15 cm². Some attention should be drawn to the area pointed to by arrows (A) in Fig. 6. Here the Bohmian-like trajectories change directions dramatically. A possible mechanism of such a deviation of the trajectories can be as follows [1, 4]: (i) the droplet moving through a slit induces a Faraday wave; (ii) velocity of the wave is an order of magnitude larger than the velocity of the droplet; (iii) for that reason the Faraday wave has time to reach the second slit; (iv) it induces a secondary Faraday wave from this slit; (v) the latter has time to reach the area pointed by arrow (A). Because of this the wave brings a correction in the motion of the droplet in the vicinity of this place. Both primary and secondary waves, in the superposition, play a role of the guiding wave. It should be noted that there are no intersections of the Bohmian trajectories with each other as they go on. Intersections of traces shown in a figure in [1] are in contradiction with the ideas of de Broglie and Bohm [18, 29, 30].

IV. CONCLUSION.

Droplets bouncing on a vibrating silicon oil surface behave themselves as particles, if the vibrations are supported slightly below the Faraday instability threshold. Such vibrations are akin to zero-point vacuum oscillations. In this case we may use the Feynman path integral to study interference effects induced by moving droplets through obstacles having slits. However, instead of the Planck constant we need to use a surrogate parameter which is material dependent and also depends on the forcing oscillations and the size of the droplets.

In the vicinity of the Faraday instability threshold the oil surface is very sensitive to weak

contacts. Owing to nearness to the Faraday instability threshold, excited waves are long-lived. It is manifestation of a memory effect on the moving bouncing droplet [4]. Superposition of such excited waves makes the de Broglie pilot wave [14] guiding the droplet along an optimal path.

Basic foundation for description of the de Broglie pilot wave goes back to the equations of Navier-Stokes and the conservation of mass. In approximation of the irrotational incompressible fluid these two equations are reduced to the nonlinear Schrödinger equation, wherein the surrogate parameter is used instead of the Planck constant. Its wave solutions are determined by boundary conditions imposed on a problem under consideration, among which a grating with slits plays the crucial role. The latter gives a Fourier image of the grating in the far-field, which forms a virtual interference pattern from the slits. In turn, the moving droplet generates circular waves at each impact with the fluid surface. These waves, having a greater velocity of spreading, bring the interference pattern

along the motion of the droplet. It directs the droplet motion along the optimal path - along the Bohmian trajectory.

We have shown that (a) the Navier-Stokes equation together with the continuity equation can be reduced to the Schrödinger equation assuming an incompressible irrotational fluid; (b) the Feynman path integral underlying the Schrödinger equation can be applied for finding droplet's paths through a grating containing slits; (c) interference patterns arising behind the grating were calculated for two wavelengths given in [1] - $\lambda = 4.75$ mm and $\lambda = 6.95$ mm.

Experiments with droplets bouncing on surface of a fluid that undergoes the Faraday oscillations [1, 4] can shed the light on the subtle behavior of vacuum as particles pass through.

Acknowledgments

The author is gratefully acknowledged to O. A. Bykovsky and Dr. S. M. Bezrukov for interesting discussions and series of useful remarks.

-
- [1] Y. Couder and E. Fort, Single-Particle Diffraction and Interference at a Macroscopic Scale, *Phys. Rev. Lett.* 97 (2006) 154101.
 - [2] Y. Couder, E. Fort, C.-H. Gautier, and A. Boudaoud, From bouncing to floating drops: non-coalescence of drops on a fluid bath, *Phys. Rev. Lett.* 94 (2005) 177801.
 - [3] S. Protière, A. Boudaoud, and Y. Couder, Particle-wave association on a fluid interface, *J. Fluid Mech.* 554 (2006) 85-108.
 - [4] A. Eddi, E. Sultan, J. Moukhtar, E. Fort, M. Rossi, and Y. Couder, Information stored in Faraday waves: the origin of a path memory, *J. Fluid Mech.* 674 (2011) 433-463.
 - [5] G. A. Krenev, The fifth dimension? e-print, (2002) 1-4: URL http://www.sinor.ru/~bukren/kr_st1_1.htm (In Russian)
 - [6] R. P. Feynman, *Statistical Mechanics: A Set of Lectures*, (Addison-Wesley, Massachusetts 1998).
 - [7] S. Dorbolo, D. Terwagne, N. Vandewalle and T. Gilet, Resonant and rolling droplet, *New Journal of Physics*, **10** (2008) 113021
 - [8] T. Gilet, D. Terwagne, N. Vandewalle, and S. Dorbolo, Dynamics of a Bouncing Droplet onto a Vertically Vibrated Interface, *PRL* **100** (2008) 167802.
 - [9] J. Miles and D. Henderson, Parametrically forced surface waves, *Annu. Rev. Fluid Mech.* 22 (1990) 143-165.
 - [10] J. Miles, On Faraday waves, *J. Fluid Mech.* 248 (1993) 671-683.
 - [11] N. P'erinet, D. Juric, and L. S. Tuckerman, Numerical simulation of Faraday waves, *J. Fluid Mech.* 635 (2009) 1-26.
 - [12] E. Madelung, Quantumtheorie in hydrodynamische form, *Zts. f. Phys.* 40 (1926) 322-326.
 - [13] R. Guantes, A. S. Sanz, J. Margalef-Roig, S. Miret-Artés, Atom-surface diffraction: a trajectory description, *Surface Science Reports*, 53 (2004) 199-330.
 - [14] X. Oriols and J. Mompart, Overview of Bohmian Mechanics, in: Oriols X., Mompart J. (Eds.), *Applied Bohmian Mechanics from Nanoscale Systems to Cosmology*, Pan Stanford Publishing Pte. Ltd., Singapore, 2012, pp. 15-147.
 - [15] D. Bohm and J. P. Vigier, Model of the causal interpretation of quantum theory in terms of a fluid with irregular fluctuations, *Phys. Rev.* 96 (1954) 208-216.
 - [16] L. D. Landau and E. M. Lifshitz, *Fluid mechanics*, Pergamon Press, Oxford, 1987.
 - [17] E. Nelson, Derivation of the Schrödinger equation from Newtonian Mechanics, *Phys. Rev.* 150 (1966) 1079-1085.
 - [18] D. Bohm, A suggested interpretation of the quantum theory in terms of "hiddenvariables", I & II, *Phys. Rev.* 85 (1952) 166-193.
 - [19] V. I. Sbitnev, Bohmian trajectories and the path integral paradigm. Complexified Lagrangian mechanics, *Int. J. Bifurcation & Chaos*, 19 (2009) 2335-2346.
 - [20] URL <http://www.youtube.com/watch?v=5PmnaPvAvQY>
 - [21] R. P. Feynman, Space-Time approach to non-relativistic

- quantum mechanics, *Rev. Mod. Phys.* 20 (1948) 367-387.
- [22] R. P. Feynman and A. Hibbs, *Quantum Mechanics and Path Integrals*, (McGraw Hill, N. Y. 1965).
- [23] D. Derbes, Feynman's derivation of the Schrödinger equation, *Am. J. Phys.*, **64**(7), (1996) 881-884.
- [24] V. I. Sbitnev, Matter waves in the Talbot-Lau interferometry, e-print 1005.0890v3 (17 Sep 2010): URL <http://arxiv.org/abs/1005.0890>
- [25] V. I. Sbitnev, Bohmian trajectories and the path integral paradigm - Complexified Lagrangian mechanics, in: Pahlavani M. R. (Ed.), *Theoretical Concepts of Quantum Mechanics*, InTech, Rijeka, 2011.
- [26] V. I. Sbitnev, Generalized path integral technique: nanoparticles incident on a slit grating, matter wave interference, in: Bracken P. (Ed.), *Advances in Quantum Mechanics*, InTech, Rijeka, 2013.
- [27] A. S. Sanz and S. Miret-Artés, A causal look into the quantum Talbot effect, *J. Chem. Phys.* 126 (2007) 234106.
- [28] A. S. Sanz and S. Miret-Artés, A trajectory-based understanding of quantum interference , *J. Phys. A: Math. Gen.* 41 (2008) 435303.
- [29] L. de Broglie, *La Physique Quantique Restera-t-elle Indeterministe?*, Gauthier-Villars, Paris, 1953.
- [30] D. J. Bohm, B. J. Hiley, The de Broglie Pilot Wave Theory and the further development of new insights arising out of it, *Foundations of Physics*, 12 (1982) 1001-1016.